



CHORUS

This is the accepted manuscript made available via CHORUS. The article has been published as:

Ferroelectric Control of Interface Spin Filtering in Multiferroic Tunnel Junctions

J. Tornos, F. Gallego, S. Valencia, Y. H. Liu, V. Rouco, V. Lauter, R. Abrudan, C. Luo, H. Ryll, Q. Wang, D. Hernandez-Martin, G. Orfila, M. Cabero, F. Cuellar, D. Arias, F. J. Mompean, M. Garcia-Hernandez, F. Radu, T. R. Charlton, A. Rivera-Calzada, Z. Sefrioui, S. G. E. te Velthuis, C. Leon, and J. Santamaria

Phys. Rev. Lett. **122**, 037601 — Published 22 January 2019

DOI: [10.1103/PhysRevLett.122.037601](https://doi.org/10.1103/PhysRevLett.122.037601)

Ferroelectric control of interface spin filtering in multiferroic tunnel junctions.

J. Tornos*¹, F. Gallego *¹, S. Valencia², Y. H. Liu^{3,4}, V. Rouco⁵, V. Lauter³, R. Abrudan^{2,6}, C. Luo^{2,7}, H. Ryll², Q. Wang⁴, D. Hernandez-Martin¹, G. Orfila¹, M. Cabero¹, F. Cuellar¹, D. Arias^{1,#}, F. J. Mompean^{8,9}, M. Garcia-Hernandez^{8,9}, F. Radu², T. R. Charlton¹⁰, A. Rivera-Calzada^{1,9}, Z. Sefrioui^{1,9,11}, S. G. E. te Velthuis⁴, C. Leon^{1,9,11}, and J. Santamaria^{1,9,11}.

¹ GFMC, Universidad Complutense de Madrid, 28040 Madrid, Spain.

² Helmholtz-Zentrum Berlin für Materialien und Energie, Albert-Einstein-Strasse 15, 12489 Berlin, Germany

³ Neutron Scattering Division, Oak Ridge National Laboratory, Oak Ridge, Tennessee 37831, USA

⁴ Materials Science Division, Argonne National Laboratory, Argonne, Illinois 60439, USA

⁵ Unité Mixte de Physique, CNRS, Thales, Université Paris-Saclay, 91191 Palaiseau, France

⁶ Institut für Experimentalphysik/Festkörperphysik, Ruhr-Universität Bochum, 44780 Bochum, Germany

⁷ University of Regensburg, Universitätsstraße 31, 93053 Regensburg, Germany

⁸ 2D-Foundry Group, Instituto de Ciencia de Materiales de Madrid ICMM-CSIC, 28049 Madrid, Spain

⁹ Unidad Asociada UCM/CSIC, "Laboratorio de Heteroestructuras con aplicación en spintrónica"

¹⁰ ISIS, Rutherford Appleton Laboratory, Chilton, Oxon OX11 0QX, United Kingdom

¹¹ GFMC, Instituto de Magnetismo Aplicado, Universidad Complutense de Madrid, 28040 Madrid, Spain

ABSTRACT

The electronic reconstruction occurring at oxide interfaces may be the source of interesting device concepts for future oxide electronics. Among oxide devices, multiferroic tunnel junctions are being actively investigated as they offer the possibility to modulate the junction current by independently controlling the switching of the magnetization of the electrodes and of the ferroelectric polarization of the barrier. In this paper we show that the spin reconstruction at the interfaces of a $\text{La}_{0.7}\text{Sr}_{0.3}\text{MnO}_3 / \text{BaTiO}_3 / \text{La}_{0.7}\text{Sr}_{0.3}\text{MnO}_3$ multiferroic tunnel junction is the origin of a spin filtering functionality which can be turned on and off by reversing the ferroelectric polarization. The

ferroelectrically controlled interface spin filter enables a giant electrical modulation of the tunneling magnetoresistance between values of 10% and 1000%, that could inspire device concepts in oxides based low dissipation spintronics.

The emergent electronic states nucleating at the interfaces between correlated oxides have high technological potential [1-5] for growing “oxide electronics”, but the promise of novel device concepts has not been fulfilled yet, partly due to the insufficient understanding of the complex electronic interactions taking place [3]. The electronic and orbital reconstructions occurring at oxide interfaces underlie deep changes in their magnetic states. In particular, in perovskite oxides with an orbital moment quenched by the octahedral crystal field, magnetism is largely determined by the spin degree of freedom. Modified orbital filling stemming from charge transfer processes and/or changes in orbital overlap between distorted bonds at interfaces, drastically affect spin-spin interactions in a way captured by the Goodenough-Kanamori rule [6,7]. Interfacially induced magnetism at oxide interfaces can be used to tailor novel functionalities in magnetic tunnel junctions.

Magnetic tunnel junctions with ferroelectric barriers have focused much interest due to the possibility of modulating the tunneling current by the orientation (up or down) of the ferroelectric polarization. Tunneling electroresistance (TER) measures the change of the junction resistance when polarization is reversed [8]. TER has been theoretically discussed [9] to originate either from changes in interface bonds associated with ferroelectric polarization switching and/or from modulations of the tunnel barrier height resulting from screening asymmetries at both electrodes. A giant electroresistance has been reported [10- 17] for ferroelectric tunnel junctions with (different) metal electrodes having different screening lengths. Moreover, a relatively weak modulation of the tunneling

magnetoresistance with the ferroelectric polarization has been explained in terms of the modification of the interface spin polarization by ferroelectric field effect [18].

In this paper we show that the spin reconstruction at the interfaces of an all-oxide multiferroic tunnel junction with half metallic $\text{La}_{0.7}\text{Sr}_{0.3}\text{MnO}_3$ (LSMO) electrodes and a BaTiO_3 (BTO) ferroelectric (FE) barrier acts as a tunable spin filter which can be turned on and off by reversing the ferroelectric polarization. This enables an electrical modulation of the tunneling magnetoresistance by two orders of magnitude between 10% and 1000%. This offers an interesting route for the ferroelectric field effect control of the interfacial magnetism at the electrodes of a magnetic tunnel junction, a functionality which is actively pursued for developing low dissipation spintronics [19].

We have grown $\text{La}_{0.7}\text{Sr}_{0.3}\text{MnO}_3$ (8 nm) / BaTiO_3 (4nm) / $\text{La}_{0.7}\text{Sr}_{0.3}\text{MnO}_3$ (25 nm) epitaxially deposited onto (001) oriented SrTiO_3 (STO) substrates at elevated temperatures (750 °C), using a high pressure sputtering technique in pure oxygen atmosphere [20, 21]. Interfaces were atomically sharp both structurally and chemically as previously shown by high resolution electron microscopy STEM (HAADF) imaging and (EELS) elemental maps with both interfaces showing a symmetric $\text{LaSrO}/\text{TiO}_2$ termination [22]. Piezoelectric force microscopy (PFM) using amplitude and phase contrast on BTO/LSMO bilayers indicated a ferroelectric ground state and the possibility to ‘write’ up or down polarization states using a few volts tip bias [22]. Micron-sized pillars were fabricated by using conventional optical lithography techniques and Ar ion milling. An initial ferroelectric domain state stabilized by native oxygen vacancies produced very weak piezoelectric contrast in the patterned pillars, but a homogeneous polarization state was stabilized after the initial application of a few volts bias voltages. IV curves were non-linear as expected from the tunneling transport across the ultrathin ferroelectric barrier and exhibited a clear signature of polarization switching (Figure 1). Cycling the bias voltage between -5 and +5 V we have observed a clear hysteretic behavior at low voltage (10 mV) which evidences a small (200%)

electroresistance associated with polarization switching (See lower inset in Figure 1). Otherwise, at high voltage, IV curves are reversible and non-hysteretic.

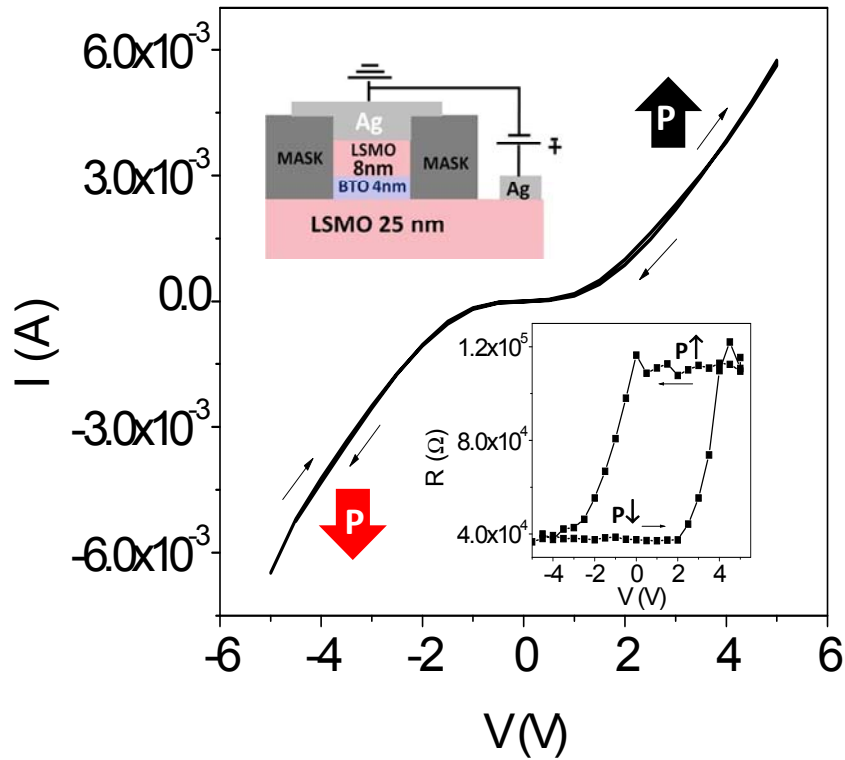


Figure 1. Main panel. Hysteretic IV curves of a LSMO/BTO/LSMO tunnel junction measured at 120 K and up to ± 5 V bias voltages to ensure the switching of the ferroelectric polarization (marked with black-up- and red -down- arrows). The sketch illustrates the sequence and thicknesses of the individual layers of the device. Bottom inset. Electroresistance loops measured at 10 mV after exciting with the continuous voltages displayed in the x axis.

This indicates that although polarization switching may be accompanied by migration of native oxygen vacancies (detected previously [22]) from one interface to the other, there is no generation of *new* oxygen vacancies which would produce characteristic irreversibilities in the resistive switching processes. The finding of electroresistance indicates a certain degree of interface asymmetry [9] as also

does the imprint (shift) of the electroresistance loop towards positive voltages (see inset of figure 1) suggesting a preferred down orientation of the ferroelectric polarization.

Magnetism of the individual layers and its profile at the interfaces was examined by combined resonant x-ray absorption and polarized neutron reflectometry on twin samples with the same layer sequence as those patterned into junction devices and discussed later. See sketch in Figure 2 (a). X-ray absorption spectroscopy (XAS) measurements were carried out at Bessy II (HZB, Berlin) with Alice diffractometer at the PM3 beamline (data not shown) and with the VEKMAG end station [23] installed at the PM2 beamline (data shown in Fig. 2(b)). To probe both manganite layers simultaneously the sample, LSMO_{top} (3 nm)/BTO (4nm)/ LSMO_{bot} (10 nm), had reduced thickness of the manganite layers which gives rise to larger coercivities. Magnetism of the manganite layers was tracked measuring the magnetic circular dichroic contrast across the Mn $L_{2,3}$ absorption edges by x ray magnetic scattering (XRMS). XRMS hysteresis loops, see Figure 2 (b), show two different coercive fields corresponding to top and bottom manganite layers which switch at different magnetic fields due to their different thicknesses. The lower coercivity corresponds to the thicker bottom manganite layer. We also found a magnetic signal at Ti $L_{2,3}$ edges, see Figure 2 (b), which we ascribe to a magnetic moment induced at the interfacial Ti due to the Ti-O-Mn superexchange interaction [24]. Ti magnetism thus closely tracks the magnetic state of the manganite layers at their interfaces with the BTO barrier. Although, the reflectivity (XRMS) mode can be affected by phase factors and cannot thus be used to quantify magnetic moment, notice that the coercivity of the Ti matches that of the Mn bottom layer and that there is not a clear coercive field in the Ti hysteresis loop corresponding to the top interface. Ti moment at the bottom interface indicates electron doping associated to the presence of oxygen vacancies.

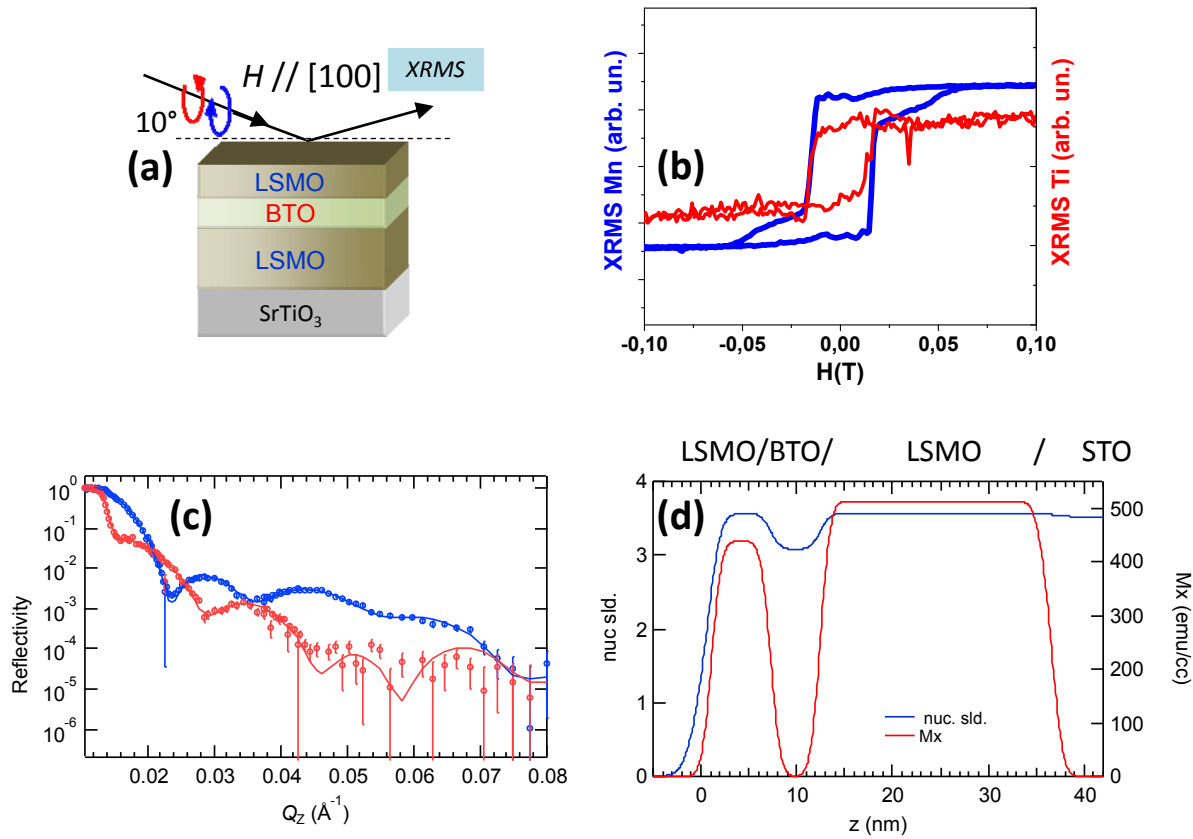


Figure 2. (a) Sketch. Layer sequence of the samples used for the x-ray absorption and neutron reflectometry experiment. (b) X-ray magnetic scattering (XRMS) hysteresis loops measured at Mn (641.4 eV) and Ti (464.6 eV) selected energies at the L 2,3 edge of a LSMO_{top} (3 nm)/BTO (4nm)/LSMO_{bot.} (10 nm) sample. Both loops were measured at 10 K with magnetic field applied in the [100] direction. (c) Polarized neutron reflectometry spectra at 10 K and an applied field of 1T of a LSMO_{top} (8 nm)/BTO (4nm)/LSMO_{bot.} (25 nm) sample. (d) The depth profile of the nuclear scattering length density and magnetization, that corresponds to the fit (lines) of the data (markers). No intentional polarization state was set, although samples displayed a preferred polarization down state.

Further information about the magnetic depth profile was obtained from Polarized Neutron Reflectometry (PNR) analysis [25], now on samples with the same manganite thicknesses as those patterned into junction devices. These measurements were performed at the Magnetism Reflectometer at the Spallation Neutron Source at Oak Ridge National Laboratory. Figure 2 (c) displays the R^+ and R^- reflectivities (incident neutron polarization parallel and antiparallel to the applied field). Lines are fits to a model that consists of a depth profile of the structural (nuclear scattering length density) and magnetic (magnetization) parameters for each defined layer (Figure 2 (d)). The top (439 emu/cm^3) and bottom (513 emu/cm^3) LSMO had different saturation magnetizations. Reduced Curie temperature of

the top interface has been assessed by neutron scattering experiments on bilayer samples (not shown). Suppressed magnetization and reduced Curie temperature, frequently found at manganite interfaces [26], is possibly due to the preferential nucleation of oxygen vacancies and may explain the suppression of Ti moment at the top interface. PNR experiments at low fields unequivocally show that the lower coercive field always corresponds to switching of the bottom manganite layer.

We measured the resistance of magnetic tunnel junctions as a function of magnetic field, which was applied along the [110] easy axis and was swept in a hysteresis loop sequence. The resistance displays abrupt switches at magnetic field values corresponding to the coercivities of bottom and top electrodes. Tunnel magneto-resistance ($TMR = (R_{AP} - R_P) / R_P$) was computed from resistance vs. magnetic field ($R(H)$) sweeps [27] and also from $I(V)$ curves acquired in the parallel (R_P) and antiparallel (R_{AP}) magnetic configurations [28]. Both methods showed very good agreement. TMR was measured as a function of bias and temperature after applying electric fields to select either up or down orientation of the ferroelectric polarization. Markedly different results were obtained in both situations. Polarization pointing up produced large TMR values approaching 1000% at low temperatures which are among the largest TMR values ever reported for magnetic tunnel junctions. On the other hand, polarization pointing down yielded much lower values of the TMR (of the order of 10%). See Figure 3. Interestingly, a non monotonic bias dependence of the TMR with voltage is observed when ferroelectric polarization is pointing down (see inset of Figure 3 (a)). On the other hand, when polarization points up TMR showed the usual monotonic decrease when bias (of either sign) was increased (see inset of Figure 3 (b)). Despite the small TER (200 %) found in our devices with symmetric interfaces, polarization switching causes a large modulation of the TMR which can be described with the tunneling electro-magneto-resistance TEMR [18] of $10^4\%$, much larger than the 450% found in Fe/BTO/LSMO samples [18] or the 900% found in Co/PbTiO₃/LSMO [29].

Polarization switching had also deep effects on the shape of the tunneling barrier, which were analyzed using the Brinkman model. When polarization is pointing up the barrier obtained is 3.6 nm thick and 0.2-0.3 eV high, while down polarization produced 2 nm thick barriers of a larger heights of 0.7 eV. This indicates that polarization switching has an effect on the ionization of oxygen vacancies which changes the position of the Fermi level and consequently of the barrier height. The larger barrier height and lower width for down-polarization suggests an increase in the ionization of oxygen vacancies remaining at the top interface, probably by electron transfer to the bottom interface to help compensating polarization charges, what in its turn reduces barrier width. This effect does not happen when polarization points up because there are no remaining vacancies at the bottom interface. [30]

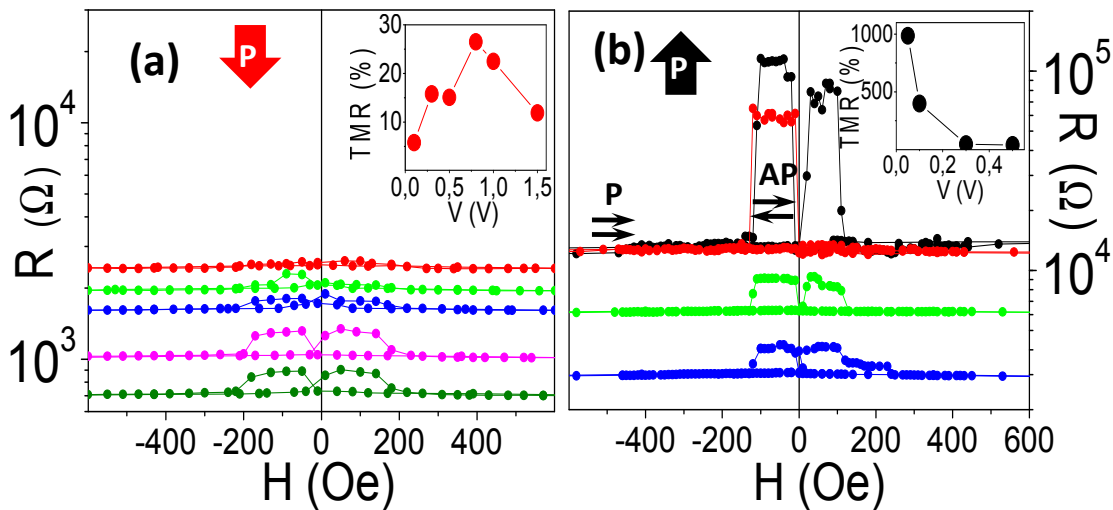


Figure 3. Resistance (R) vs. magnetic field (H), R(H) loops measured at 14 K with ferroelectric polarization pointing down (panel (a)) and ferroelectric polarization pointing up (panel (b)). Notice the semi-logarithmic scale used due to the large values of the TMR for ferroelectric polarization pointing up. Bias voltages are 0.1 V (red), 0.3 V (green), 0.5 V (blue), 0.8 V (magenta) and 1 V (olive) in panel (a) and 0.05 V (black), 0.1 V (red), 0.3 V (green), 0.5 V (blue) in panel (b). The insets illustrate the dependence of the TMR with voltage for both orientations of the ferroelectric polarization.

Figure 4 (main panel) shows the temperature dependence of the TMR measured at a voltage of 100 mV for both orientations of the ferroelectric polarization. A first observation is that the TMR decreases strongly when temperature is increased, vanishing at temperatures slightly above 100 K, which is substantially below the Curie temperature of individual manganite layers of the same thickness and growth conditions. This results from the reduced Curie temperature of the top interface which dominates the onset temperature of the spin-dependent tunneling. The small panels in Fig 4 display the bias dependence of the TMR as measured from IV curves and highlight that the low temperature suppression of TMR and non monotonic bias dependence occur consistently for ferroelectric polarization pointing down (red lines), while for polarization pointing up (black lines) the usual monotonic dependence of TMR with bias is recovered.

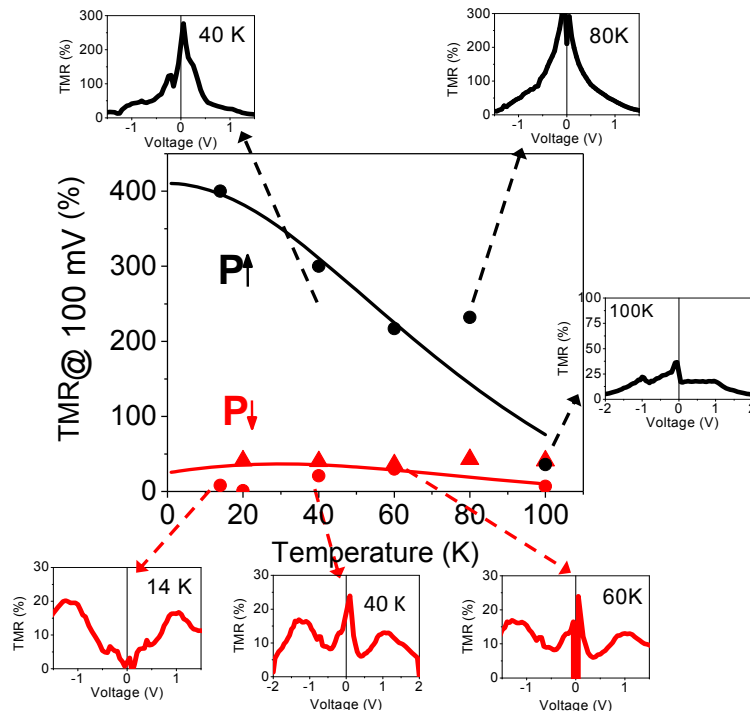


Figure 4. Temperature dependence of the tunneling magnetoresistance TMR measured at 100 mV voltage for ferroelectric polarization pointing up (black symbols) and down (red symbols). Circles and triangles correspond to two different samples. Lines are fits to the spin filtering model (see text). Small panels display the bias dependence of the TMR at selected temperatures as obtained from IV curves measured in parallel and antiparallel states. Notice the monotonic bias dependence for polarization pointing up and the non-monotonic dependence for polarization pointing down.

The temperature dependence of the TMR (main panel in Fig. 4) is markedly different for both orientations of the ferroelectric polarization. For polarization pointing up, TMR increases monotonically when the temperature is decreased, as expected from the commonly observed growth of spin polarization. On the other hand, for polarization pointing down, there is a suppression of the TMR at low temperatures which is characteristic of spin filters.

Spin filtering was first introduced by Esaki [37] and later demonstrated in junctions with ferromagnetically insulating barriers and superconducting [38] or ferromagnetic [39, 40] electrodes. Spin filtering obeys to the different barrier heights for majority and minority spins what triggers different transmission probabilities for both spin channels thus spin polarizing the tunneling current. In conventional magnetic tunnel junctions TMR is known to decrease monotonically with increasing bias and temperature due to the excitation of magnons [41] which cause spin mixing. However, in spin filters TMR does not depend monotonically on bias showing a pronounced increase at the onset of the Fowler-Nordheim FN regime [42] due to the enhanced transmission for one spin channel. IV curves for the down orientation of the polarization showed two sequential FN processes which indicates spin splitting of the barrier [30].

We propose that in our case spin filtering stems from the Ti magnetic moment induced at the interface. Ti magnetism results from oxygen vacancies which dope electrons into the Ti^{3+} state. Ti orbitals hybridize with Mn orbitals according to the hierarchy sketched in Figure 5. The Ti-O-Mn superexchange path across the interface enabled by the LaSrO/ TiO_2 terminations is responsible for the antiparallel alignment between Ti and Mn moments [24]. I.e., the antiparallel Ti moment naturally follows from the hybridization of unpolarized degenerate Ti xz and yz orbitals with the corresponding down spin t_{2g} hybrids of the Mn (notice that the spin up t_{2g} hybrids splitted by the large Hund coupling interaction of the manganite are filled with the Mn t_{2g} electrons) [43, 44]. Ti magnetism has been also theoretically

proposed previously in Fe/ BTO interfaces resulting from the (polarization modulated) hybridization of Ti orbitals with Fe spin down band [45].

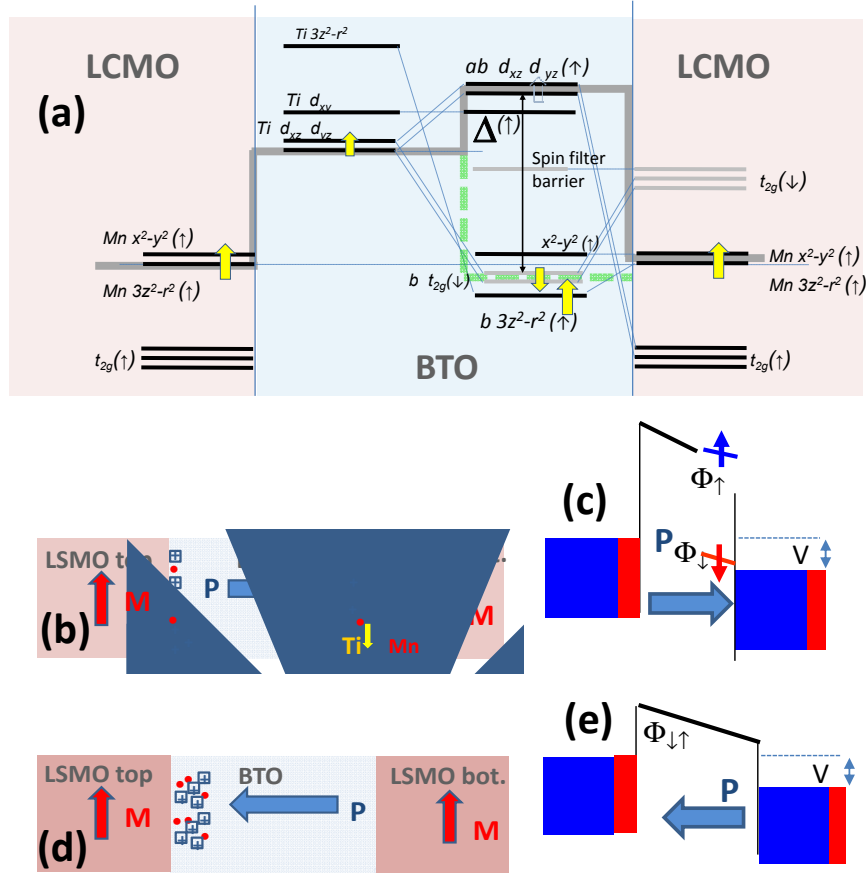


Figure 5. (a) Orbitals scheme of the manganite/titanate bonding at the interface. We do not show electrons in the t_{2g} orbitals of the manganite. For clarity we have only illustrated bonding at the right interface. The unpolarized dx_z and dy_z bands hybridize with spin up and down t_{2g} band splitted by the exchange interaction of the manganite. The thick grey line shows the profile of the spin up conduction band in the z direction relevant for the tunneling transport in of the device. Sketches illustrating the alternative electron doping of bottom (panel (b)) and top interfaces (panel (d)) due to the simultaneous switching of ferroelectric polarization and oxygen vacancies. The Ti magnetism occurring preferentially at the bottom interface has a negative spin filtering functionality (panel (c)) not occurring at the top interface (panel (e)).

The spin split interface barrier results then from the energy difference between the spin down bonding-hybrids (marked with dotted green line) and the higher energy dx_z/yz spin up anti bonding- hybrid

(marked with continuous grey line). Spin down hybrids are lower in energy than spin up hybrids due to the stronger hybridization of the former. See sketch in Figure 5 (a).

The larger barrier height for spin up than for spin down electrons has a direct implication on the transmission probability across the tunneling barrier and accounts for the spin filtering effect (see sketch in Figure 5 (c)). We have modelled the temperature dependence of the TMR following the model proposed by Liu *et al* [46] (see lines in Figure 4) considering that, for polarization pointing down, a spin splitting of 0.3 eV at 0 K occurs at the bottom interface due to accumulation of electrons and extends over $d = 1.6$ nm. [30]. The exchange splitting is driven by spin polarization of the electrode and is assumed to be proportional to it in the model. When temperature decreases, the increase in the exchange splitting of the barrier causes a reduction of the effective polarization of the tunnelling current and is thus responsible for the non-monotonic decrease of the TMR [46, 47].

Finally we discuss the suppression of the spin filtering effect when polarization is switched up. The induced Ti magnetic moment responsible for the spin filtering is due to the metallization of the bottom interface. Electron doping of the bottom interface by vacancies preferentially nucleating at the top interface naturally explains the preferred down orientation of the ferroelectric polarization indicated by the imprint observed in the electroresistance loops although we cannot discard partial switching of oxygen vacancies simultaneous to polarization switching [22] (see sketch in Figure 5 (b)). Interfacial Ti magnetism with a spin filtering effect is induced only at the bottom interface due to the robust magnetism of the bottom manganite electrode. See sketch in Figure 5 (b) and (c). The depressed interface magnetism (frequently encountered in manganites [26]) denounced by its reduced Curie temperature, breaks the interfacial superexchange path weakening (or suppressing) Ti magnetism and thus spin filtering does not occur when polarization is directed towards the upper interface. See sketch in Figure 5 (d) and (e).

In summary, we have demonstrated a very large ferroelectric modulation of the tunneling magnetoresistance of a multiferroic tunnel junction, driven by an interfacially induced spin filtering functionality. Spin filtering is triggered by the induced spin polarization of the ferroelectric interface, probably by accumulation of oxygen vacancies, which yields a Ti^{3+} species bonding to Mn across a Mn-O-Ti superexchange path. The ferroelectric control relies in asymmetries in the magnetic structure of the interfaces. The very large modulation of the TMR between 10 and 1000%, enabled by the emergent spin filter calls for future strategies for the design of wider classes of interfacial spin filters exploiting electronic reconstruction at oxide interfaces.

Acknowledgments

Work supported by Spanish MINECO through grants MAT2014- 52405-C02, MAT2017-87134-C02, MAT2015-72795-EXP and CAM S2013/MIT-2740. Work at Argonne National Laboratory (PNR experiments and analysis) was supported by the U.S. DOE, Office of Science, Basic Energy Sciences, Materials Sciences and Engineering Division. Neutron scattering experiment was conducted at the Spallation Neutron Source, a DOE Office of Science User Facility operated by the Oak Ridge National Laboratory. Beamtime support provided at Alice (BMBF project No. 05K10PC2) is acknowledged. Financial support for developing and building the PM2-VEKMAG beamline and VEKMAG end station was provided by HZB and BMBF (05K10PC2, 05K10WR1, 05K10KE1), respectively. Steffen Rudorff is acknowledged for technical support. JS thanks Scholarship program Alembert funded by the IDEX Paris-Saclay, ANR-11-IDEX-0003-02.

REFERENCES

* These authors have contributed equally to this work

On leave from Universidad del Quindío. Armenia. Colombia

[1] Mannhart, J. & Schlom, D. G. *Science* 327,1607 (2010).

[2] Hwang, H. Y. *et al.* *Nature Materials* 11, 103 (2012).

[3] J. Chakhalian, A.J. Millis and J. Rondinelli *Nature Materials* 11, 92 (2012)

[4] Ngai, J. H., Walker, F. J. & Ahn, C. H. *Annu. Rev. Mater. Res.* 44, 1 (2014).

[5] Zubko, P., Gariglio, S., Gabay, M., Ghosez, P. & Triscone, J. *Annu. Rev. Condens. Matter Phys.* 2, 141 (2011).

[6] J. B. Goodenough, *Phys. Rev. B* 100, 564-573 (1955).

[7] J. Kanamori, *J. Phys. Chem. Solids* 10, 87-98 (1959).

[8] J. P. Velev, C.-G. Duan, J. D. Burton, A. Smogunov, M. K. Niranjani, E. Tosatti, S. S. Jaswal, and E. Y. Tsymbal, *Nano Lett.*, **9**, 427, (2009)

[9] M. Y. Zhuravlev, R. F. Sabirianov, S. S. Jaswal, and E. Y. Tsymbal, *Phys. Rev. Lett.* 94, 246802 (2005); E. Tsymbal and H. Kohlstedt, *Science* **313**, 181 (2006).

[10] V. Garcia , S. Fusil , K. Bouzehouane , S. Enouz-Vedrenne, N. D. Mathur , A. Barthélémy , M. Bibes , *Nature* **460** , 81 (2009) .

[11] P. Maksymovych , S. Jesse , P. Yu , R. Ramesh , A. Baddorf, S. V. Kalinin , *Science* **324** , 1421 (2009) .

[12] A. Gruverman , D. Wu , H. Lu , Y. Wang , H. W. Jang , C. M. Folkman, M. Rzchowski , C.-B. Eom , E. Y. Tsymbal , *Nano Lett.* **9** , 3539 (2009) .

[13] D. Pantel , S. Goetze , D. Hesse , M. Alexe , *ACS Nano* **5** , 6032 (2011) .

- [14] D. Pantel , H. Lu , S. Goetze , P. Werner , D. J. Kim , A. Gruverman, D. Hesse , M. Alexe , *Appl. Phys. Lett.* **100** , 232902 (2012) .
- [15] D. Pantel , S. Goetze , D. Hesse , M. Alexe , *Nat. Mater.* **11** , 289 (2012).
- [16] L. Jiang , W. S. Choi , H. Jeon , S. Dong , Y. Kim , M.-G. Han , Y. Zhu , S. Kalinin , E. Dagotto , T. Egami , H. N. Lee , *Nano Lett.* **13** ,5837 (2013)
- [17] Z. Wen , C. Li , D. Wu , A. Li , N. Ming , *Nat. Mater.* **12** , 618 (2013).
- [18] V. Garcia et al. *Science* **327** 1106 (2010).
- [19] Fusil S, Garcia V, Barthélémy A, Bibes M. *Annu. Rev. Mater. Res.* **44**, 91 (2014)
- [20] M. Varela et al, *Phys. Rev. Lett.* **83**, 3936 (1999)
- [21] M. Varela, W. Grogger, D. Arias, Z. Sefrioui, C. León, C. Ballesteros, K. Krishnan y J. Santamaría, *Phys Rev. Lett.* **86**, 5156 (2001).
- [22] G. Sanchez-Santolino et al. *Nature Nanotechnology* **12**, 655 (2017)
- [23] ALICE: A diffractometer/reflectometer for soft X-ray resonant magnetic scattering at BESSY II. *Journal of large-scale research facilities*, 2, A69 (2016). VEKMAG: T. Noll and F. Radu, *Proceedings of MEDSI2016* , 370 (2017).
- [24] Yaohua Liu et al. *APL Materials* **4**, 046105 (2016)
- [25] M. R. Fitzsimmons and C. Majkrzak, in *Modern Techniques for Characterizing Magnetic Materials*, edited by Y. Zhu (Springer, New York, 2005), pp. 107–155
- [26] V. Garcia, M. Bibes, A. Barthelemy, M. Bowen, E. Jacquet, J.-P. Contour, and A. Fert *Phys. Rev. B* **69**, 052403 (2004).
- [27] Z. Sefrioui et al. *Adv. Mat.* **22**, 5029 (2010).

- [28] F. A. Cuellar et al. *Nature Communications* 5, 4215 (2014)
- [29] Zheng-Dong Luo, Geanina Apachitei, Ming-Min Yang, Jonathan J. P. Peters, Ana M. Sanchez, and Marin Alexe *Appl. Phys. Lett.* 112, 102905 (2018)
- [30] See Supplemental Material [url] for analysis of the tunneling barrier and model of spin filtering, which includes Refs. [31- 36].
- [31] J.G. Simmons. *J. Appl. Phys.* 34 1793 (1963)
- [32] W.F. Brinkman, R.C. Dynes, and J.M. Rowell, *J. Appl. Phys.* 41 1915 (1970)
- [33] M. Müller, G-X. Gao and J. Moodera, *EPL* 88, 47006 (2009)
- [34] D. C. Worledge and T. H. Geballe, *J. Appl. Phys.* 88, 5277 (2000)
- [35] Santos, T. et al. *Phys. Rev. Lett.* 101, 147201 (2008).
- [36] M. Jullière, *Phys. Lett. A* 54, 225–226 (1975).
- [37] L. Esaki, P. J. Stiles, and S. von Molnar, *Phys. Rev. Lett.* 19, 852 (1967).
- [38] J. S. Moodera, X. Hao, G. A. Gibson, and R. Meservey, *Phys. Rev. Lett.* **61**, 637 (1988)
- [39] T. Nagahama, T. S. Santos, and J. S. Moodera. *Phys. Rev. Lett.* **99**, 016602 (2007)
- [40] M. Gajek et al., *Nature Mater.* **6**, 296 (2007).
- [41] J. S. Moodera, J. Nowak, and R. J. M. van de Veerdonk, *Phys. Rev. Lett.* **80**, 2941 (1998).
- [42] R. H. Fowler and L. Nordheim, *Proc. R. Soc.* **A 119**, 173 (1928).
- [43] S. Okamoto, *Phys. Rev. B* **82** 024427 (2010).
- [44] J. Garcia-Barriocanal et al. *Nature Comm.* **1**:82 doi: 10.1038/ncomms1080 (2010).

[45] M. Fechner, I. V. Maznichenko, S. Ostanin, A. Ernst, J. Henk, P. Bruno, and I. Mertig. *Phys. Rev. B* 78, 212406 (2008)

[46] Yaohua Liu, F. A. Cuellar, Z. Sefrioui, J. W. Freeland, M. R. Fitzsimmons, C. Leon, J. Santamaria, and S. G. E. te Velthuis *Phys. Rev. Lett.* 111, 247203 (2013).

[47] F. Y Bruno, et al. *Nature Commun.* 6, 6306 ncomms 7306 (2015).